Available online at www.sciencedirect.com
SCIENCE DIRECT®
Remote Sensing of Environment 85 (2003) 475–483
Remote Sensing of Environment
www.elsevier.com/locate/rse

Seasonal and spatial distribution of chlorophyll-*a* concentrations and water conditions in the Gulf of Tonkin, South China Sea

DanLing Tang[a,b,*], Hiroshi Kawamura[a], Ming-An Lee[c], Tran Van Dien[d]

[a] *Center for Atmospheric and Oceanic Studies, Graduate School of Science, Tohoku University, Sendai, Japan*
[b] *Institute of Hydrobiology, Jinan University, Guangzhou, China*
[c] *Department of Environmental Biology & Fisheries Science, National Taiwan Ocean University, Keelung, Taiwan*
[d] *Haiphong Institute of Oceanography, Haiphong, Viet Nam*

Received 16 September 2002; received in revised form 18 December 2002; accepted 11 February 2003

Abstract

The Gulf of Tonkin is a semi-closed gulf northwest of the South China Sea, experiencing reversal seasonal monsoon. Previous studies of water conditions have been conducted in the western waters of the gulf, but very few studies of the Chlorophyll-*a* (Chl-*a*) distribution have been carried out for the entire gulf. The present study investigates seasonal and spatial distributions of Chl-*a* and water conditions in the Gulf of Tonkin by analyzing Sea-viewing Wide Field-of-View Scanner (SeaWiFS) derived Chlorophyll-*a* (Chl-*a*), in situ measurements, sea surface temperatures (SST), and other oceanographic data obtained in 1999 and 2000. The results show seasonality of Chl-*a* and SST variations in the Gulf of Tonkin, and reveal phytoplankton blooming events in the center part of the gulf during the northeast monsoon season. In summer, Chl-*a* concentrations were relatively low (<0.3 mg m^{-3}) and distributed uniformly throughout most of the area, with a belt of higher Chl-*a* concentrations along the coast, particularly the coast of Qiongzhou Peninsula; in winter, Chl-*a* concentration increased (0.5 mg m^{-3}) in the entire gulf, and phytoplankton blooms offshore-ward from the northeast coast to the center of the gulf, while Chl-*a* concentrations reached high levels (0.8–1 mg m^{-3}) in the center of the blooms. One peak of Chl-*a* concentrations was observed during the northeast monsoon season in the year. SST were high (27–29 °C) and distributed uniformly in summer, but lower with a large gradient from northeast (17 °C) to southwest (25 °C) in winter, while strong northeast winds (8–10 m/s) were parallel to the east coast of the gulf. Comparison of Chl-*a* values shows that SeaWiFS derived Chl-*a* concentrations match well with in situ measurements in most parts of the gulf in May 1999, but SeaWiFS derived Chl-*a* are higher than in situ data in river mouth waters. The seasonal variation of Chl-*a* concentrations and SST distribution were associated with the seasonally reversing monsoon; the winter phytoplankton blooms were related to vertical mixing and upwelling nutrients drawn by the northeast wind.

Keywords: Chl-*a*; Phytoplankton; SeaWiFS; AVHRR SST; Wind; Gulf of Tonkin; South China Sea

1. Introduction

The Gulf of Tonkin is a semi-closed gulf located northwest of the South China Sea. A few oceanography studies concerning water quality were conducted in the west coastal waters of the gulf, and biological process, including spatial and seasonal variation of phytoplankton concentration, have remained unknown or poorly known for most of the gulf (Penjan, Siriporn, Natinee, & Somboon, 2000; Shaw & Chao, 1994). The present study investigates monthly and spatial distributions of Chlorophyll-*a* (Chl-*a*), sea surface temperature (SST), and water conditions in the Gulf of Tonkin by examining satellite and in situ measurements.

The Gulf of Tonkin is 270 km wide, connecting with the South China Sea through the south of the gulf and the Qiongzhou Strait. It is located northwest of the South China Sea (16°10′–12°30′N, 105°40′–110°00′E) (Fig. 1A). Hainan Island is in the east part of the gulf, and the Qiongzhou Strait is about 20 km wide and 100 m deep in between the Hainan Island and the Qiongzhou Peninsula. There is a narrow continental shelf along the east coast of Hainan Island, with a depth range from 0 to 100 m (Fig. 1B). The Red River (Fig. 1A) provides the major riverine discharge into the gulf, along with some smaller rivers along the north and west coastal area. Discharge from the Pearl

* Corresponding author. Center for Atmospheric and Oceanic Studies, Graduate School of Science, Tohoku University, Sendai 980-8578, Japan. Tel.: +81-22-217-6744; fax: +81-22-217-6748.
E-mail address: lingzis@ocean.caos.tohoku.ac.jp (D.L. Tang).

0034-4257/03/$ - see front matter © 2003 Elsevier Science Inc. All rights reserved.
doi:10.1016/S0034-4257(03)00049-X

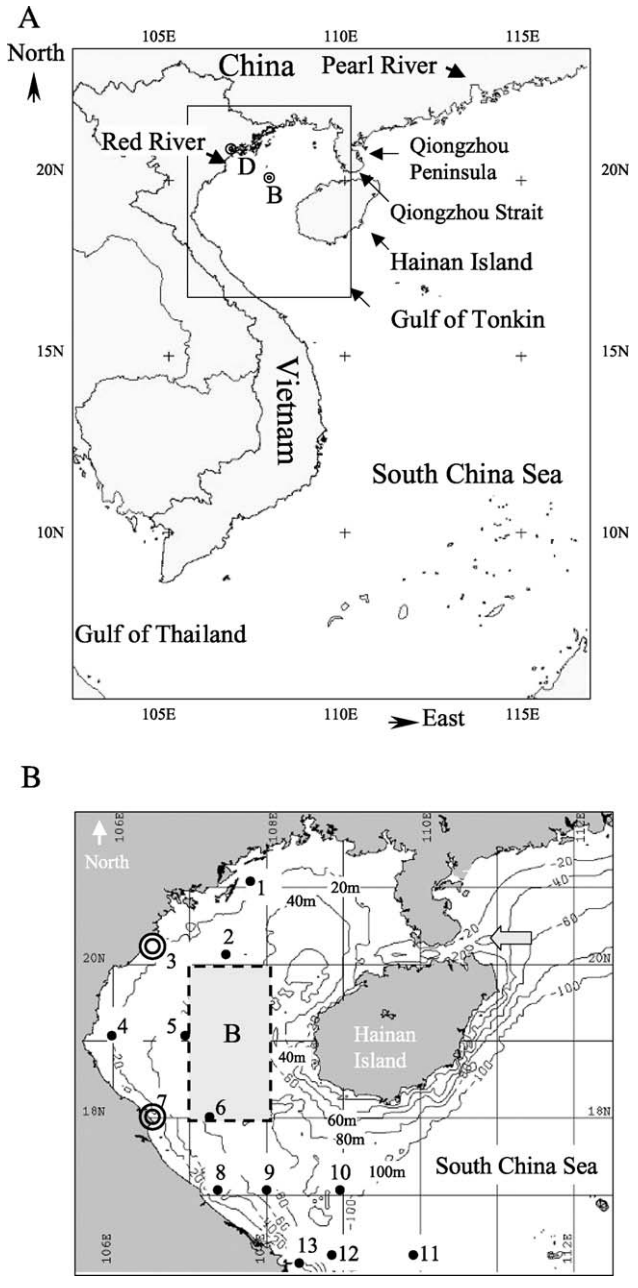

Fig. 1. (A) Geography of the study area (small box). D: Do Son station. B: Banh Long Vy station. (B) The bathymetric chart of study area with 13 sapling stations. Box B shows the SeaWiFS data sampling area.

River about 400 km to the northeast may reach the gulf through the Qiongzhou Strait (Fig. 1B).

The seasonally reversing monsoon wind plays an important role in hydrological features and the general circulation in the study region. In the South China Sea, the beginning of northeast monsoon (winter season) is in September, the first appearance of the southwest monsoon is in May, and expands to cover the entire basin during July and August (Shaw & Chao, 1994). A Vietnam–China integrated survey was carried during 1961–1964, and the Southeast Asian Fisheries Development Center Cruise (SEAFDEC) made a survey for the west coastal water in May 1999 (Penjan et al., 2000). Unfortunately, these surveys were limited to the western coastal waters, without covering the entire gulf. Numerical simulation models of the South China Sea reported the strongest current (>40 cm/s in velocity) in the Qiongzhou Strait and the sea area southwest of the Hainan Island (Huang, Wang, & Chen, 1994). Knowledge of the marine biology and oceanic processes is lacking for this area, particularly for the northeast part of the gulf.

Remote sensing with repeated coverage is the most efficient method to monitor and study the marine environment. Satellite ocean color imagery has been used to estimate Chl-*a* concentrations as an indicator of phytoplankton abundance. Coastal Zone Color Scanner (CZCS), Seaview Wide Field-of-view Sensor (SeaWiFS) ocean color images, and Advanced Very High Resolution Radiometer (AVHRR) data have been utilized for research on marine biological progresses and environmental research in the coastal waters of the South China Sea (Tang & Kawamura, 2002; Tang, Kester, Ni, Kawamura, & Hong, 2002; Tang, Ni, Müller-Karger, & Liu, 1998), but few studies have covered the Gulf of Tokin. Global calibration and validation of SeaWiFS data has been provided by optical buoy data (Hooker & McClain, 2000), but there have been no studies on validation of SeaWiFS derived Chl-*a* for the Gulf of Tonkin.

Previous studies showed high pigment concentrations northeast of the Gulf of Tonkin when we examined CZCS images along the continental shelf of China for the period from 1978 to 1986 (Fig. 2) (Tang et al., 1998). The pigment concentrations, including Chl-*a*, Chl-*b*, plus phaeopigments and dissolved organic matters, reached 1 mg m^{-3} in the center of the gulf in November 1979, which indicated high phytoplankton content in this region. These observed high phytoplankton levels were not associated with the mouths of Red or Pearl Rivers, but they were located in the northeast

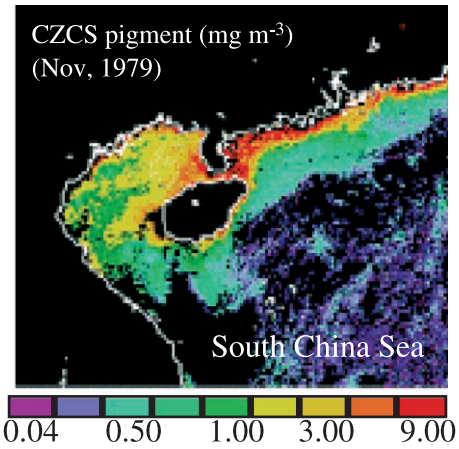

Fig. 2. Monthly composite CZCS image in November 1979 showing high pigment concentrations in the Gulf of Tonkin. The lands and clouds are shown in black color and coastal lines in white color. Color bar indicates pigment concentrations. Spatial resolution is 4 km.

gulf and offshore toward the center of the gulf. Major questions concerning this observation are: (1) Do these high phytoplankton levels exist throughout the year or are there phytoplankton blooms of short or seasonal duration? (2) Why do these high phytoplankton occur in the center of the gulf but not near the river mouths where usually there are more nutrients? (3) What are the spatial and temporal variations of phytoplankton/Chl-*a* concentrations in the Gulf of Tonkin? The present study examines these questions using Chl-*a* values obtained from satellite remote sensing and in situ measurements in this region.

2. Data and method

2.1. Survey measurements and water monitoring

In situ Chl-*a* data were measured from 13 stations in the west part of the Gulf of Tonkin (Fig. 1B) by a SEAFDEC cruise carried out during April 29 to May 31 in 1999. The water samples of 2–5 l were collected at the surface (2 m) and pre-filtered with a plankton net of 300 μm mesh size and then vacuum filtered through G/F filters with 47 mm diameter under 10 in. of Hg in the dark. The extracted samples were run by a Thermo-separation HPLC systems (a binary gradient pump, auto-sampler, UV detector, and degasser) filled with a 5 μm HICHROMS 50 DS (4.6 × 250 mm) (Suchint & Puntip, 2000).

To compare water conditions in the coastal and central portions of the gulf, water sampling was carried out at Banh Long Vy station (B in Fig. 1A) in the center of the gulf in June 2000, and at Do Son station (D in Fig. 1A) near the western coast of the gulf in July 2000. These parameters were measured at the surface (within 1 m from the surface). Water temperatures were measured by specific purpose mercury thermometer with an accuracy of 0.1 °C. Total suspended solid (TSS) were measured using dried filter method with an accuracy of 0.1 mg l^{-1}.

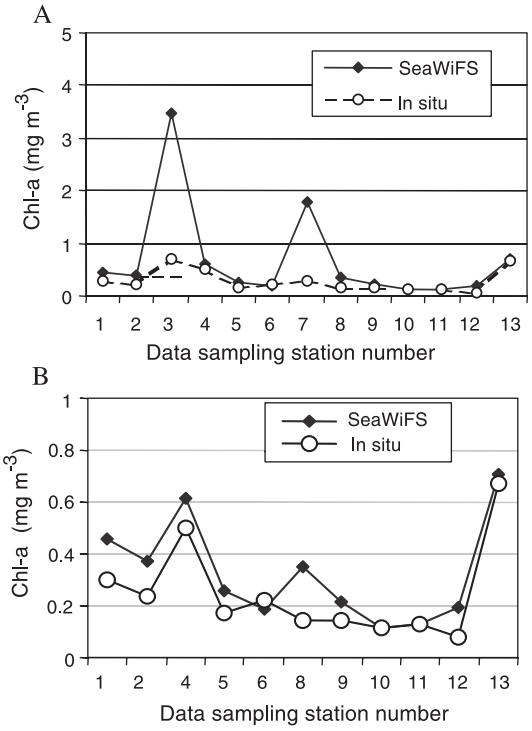

Fig. 4. Comparison between SeaWiFS derived Chl-*a* and in situ Chl-*a* obtained in the Gulf of Tonkin in May 1999. (A) Data obtained from 13 stations. (B) Data obtained from 11 stations.

2.2. SeaWiFS derived Chl-a

SeaWiFS data were obtained from the National Space Development Agency of Japan (NASDA). To display spatial distribution of Chl-*a*, we first processed SeaWiFS images and flag maps using the ocean color 4-band algorithm (OC4) (O'Reilly et al., 1998) through SeaWiFS Data Analysis System (SeaDAS) at Asian I-Lac Project (Tang & Kawamura, 2002). A total of 541 scenes with good coverage for the gulf were selected to process Chl-*a* image

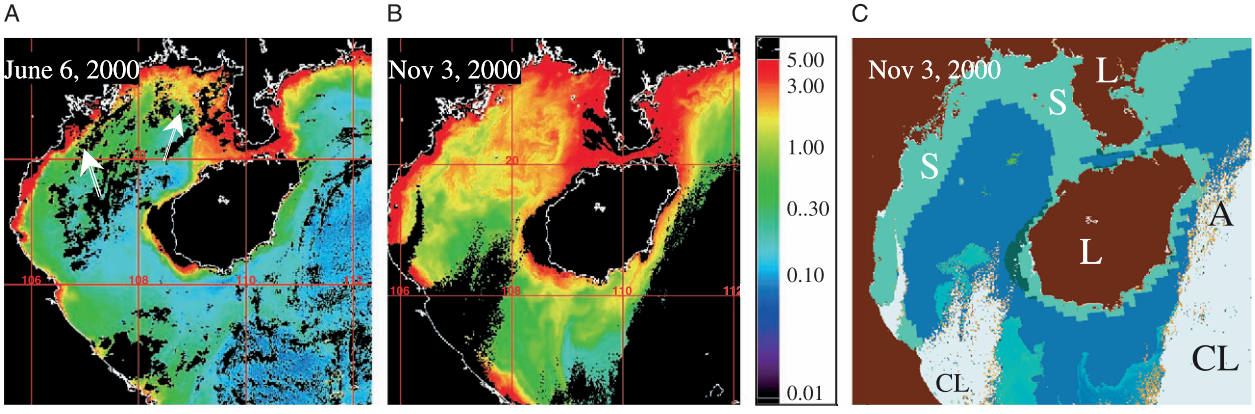

Fig. 3. SeaWiFS derived Chl-*a* images of 1 km spatial resolution. In (A) and (B), the lands and clouds are shown in black color and coastal lines in white color, color bar indicates Chl-*a* concentrations. (A) Chl-*a* on June 6, 2000. (B) Chl-*a* on November 3, 2000. (C) Flag and mask on November 3, 2000. A: high aerosol; CL: clouds; L: land; S: shallow water.

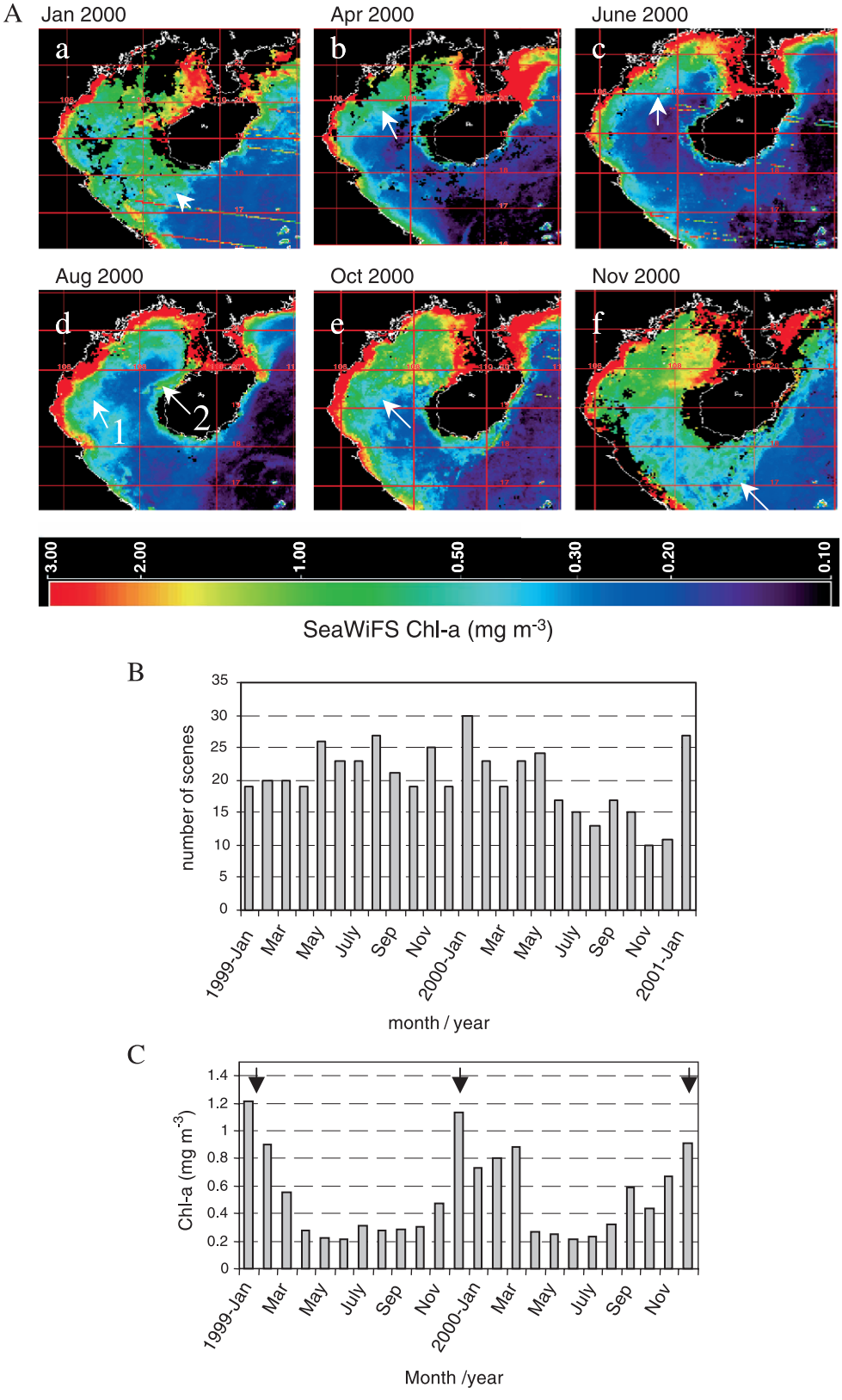

Fig. 5. (A) Monthly averaged SeaWiFS Chl-*a* images in 2000. Spatial resolution is 4 km. Color bars indicate Chl-*a* concentrations. Lands and clouds are shown in black color and coastal lines in white color. (B) Number of SeaWiFS scenes for monthly averaged images (A). (C) Monthly average of SeaWiFS derived Chl-*a* concentrations in the center part of the gulf (B in Fig. 1B) obtained during January 1999 to December 2000.

(1 km spatial resolution) in 1999 and 2000. Masks (such as land mask and cloud mask) have been applied for every image, and flags have been considered as well. We then processed monthly averaged images of 4×4 km^2 resolution for every month.

To compare SeaWiFS data with in situ measurements, we selected 13 stations at the same location as a SEAFDEC cruise survey (13 stations in Fig. 1B) to sample Chl-*a* values from the monthly averaged image (4×4 km^2) for May 1999. Average values of Chl-*a* concentration were calculated on 5×5 pixels (that is 20×20 km^2) for each station. We use a monthly image because single scene images do not have good data coverage, and the cruise took about 1 month in May.

Considering the influences of suspended sediments in the river mouth area and the reflection in shallow water along the coast, a sampling area was established in the center of the gulf (box B in Fig. 1B) (18–22°N, 107–108°E). We sampled Chl-*a* values from every monthly averaged image and then calculated a mean value for the sampling area. This sampling area covers 100×200 km, with 2664 pixels in the monthly averaged image.

2.3. AVHRR derived SST

NOAA satellites provide SST measurements from the AVHRR instruments. AVHRR images with 1.1 km spatial resolution at nadir were obtained from the satellite receiving station of the National Taiwan Ocean University (Hsu, Lee, Lee, Liao, & Lu, 2000). A total of 2349 satellite images were collected from January 2000 to January 2001. All images were navigated (i.e., corrected for distortion and registered to a map), and were nudged (i.e., the entire image shifted to fit map overlap) to correct for receiving system timing errors or satellite altitude errors. The navigation and cloud detection techniques used in this study were described by Emery, Thomas, Collins, Crawford, and Mackas (1986). Among them, the cloud-free images were further processed to obtain the multi-channel SST data (Kubota, 1994; Simpson & Humphrey, 1990). Following the geo-coordinate mapping of the images, monthly SST data were formed by arithmetically averaging all available scenes in each month on a pixel by pixel basis (excluding missing data and clouds).

2.4. QuikScat derived wind speed and direction

To describe the air–sea interaction in the study area, we analyzed sea surface wind conditions from February 2000 to January 2001 for the study area. The microwave scatterometer SeaWinds was launched on the QuikBird satellite in June 1999. QuikScat is essentially a radar device that transmits radar pulses down to the Earth's surface and then measures the power that is scattered back to the instrument. Wind speed and direction over the ocean surface are retrieved from measurements of the QuikScat backscattered power (Wentz, Smith, Mears, & Gentemann, 2001). Monthly averaged QuikScat wind vector images were produced by Remote Sensing Systems and sponsored by the NASA Ocean Vector Winds Science Team (NASA, 2001).

3. Results

3.1. Spatial distribution of Chl-a in the gulf

The spatial distribution of Chl-*a* in the Gulf of Tonkin for summer (June) and winter (November) in 2000 are illustrated by two SeaWiFS images of 1 km spatial resolution (Fig. 3A,B). In June 6, 2000 (Fig. 3A) Chl-*a* concentrations were relative low (<0.3 mg m^{-3}) and evenly distributed, high Chl-*a* concentrations were limited to a narrow zone along the coast (arrows in Fig. 3A). In November 3, 2000 (Fig. 3B) Chl-*a* concentration was much higher (>0.3 mg m^{-3}) in the entire gulf, with a gradient of higher Chl-*a* in the northeast and lower in southwest part. Some pixels along the coast are masked out where total radiances are greater than knee value, or where there were clouds. This image is consistent with the CZCS image obtained in November 1979 (Fig. 2). Fig. 3C shows the area of shallow water, high aerosol, and masks of clouds and land on November 3, 2000.

Fig. 4 shows the comparison between SeaWiFS-derived and in situ measurements of Chl-*a* obtained from 13 sampling stations (Fig. 1B) in May 1999. The shallowest station is station 4 (26 m deep), and the deepest station is station 11 (847 m in depth). Chl-*a* concentrations are high at stations 3, 7, and 13 in both SeaWiFS and in situ measurements. Both stations 3 and 7 were near the mouth of rivers, and the Chl-*a* values are higher in SeaWiFS measurements than in in situ data (Fig. 4A). When we remove these two stations from the comparison, the two data sets show better agreement (Fig. 4B).

3.2. Seasonal variation of Chl-a distribution

Details of the seasonal variation of Chl-*a* are illustrated by monthly averaged SeaWiFS images in 2000 (Fig. 5A). The number of scenes for each month is indicated by Fig. 5B.

Table 1
Water conditions at Do San station (D in Fig. 1A) and Banh Long Vy station (B in Fig. 1A) in the Gulf of Tonkin

Parameter/stations	Do Son station	Banh Long Vy station
Location	Coast area	Center of the gulf
Time	July 2000	June 2000
Temperature (°C)	30.4	29
Salinity (‰)	13.5	32.5
pH	8.14	8.11
Turbid (FTU)	5.5	1
TSS (mg/l)	10.95	14

TSS: total suspended solid.

Chl-*a* concentrations were higher in winter (November–February) (Fig. 5Aa,f) than in summer (June–August) (Fig. 5Ac,d). In winter, phytoplankton bloomed southeastward from the north coast to the center of the gulf in the beginning of November (Fig. 5Af), while Chl-*a* concentration increased (>0.3 mg m^{-3}) in the entire gulf (arrows in Fig. 5Aa,f). The bloom extends in December to February, and decreases in March. In summer, Chl-*a* concentrations were low (<0.3 mg m^{-3}) in the gulf; high Chl-*a* concentrations were limited to the coastal waters (arrows in Fig. 5Ac,d). April was a transition month, during which Chl-*a* levels were in between summer and winter, high Chl-*a* concentrations occurred in the north part of the gulf (Fig. 5Ab,e).

We observed one peak of high Chl-*a* in winter every year (January 1999, December 1999, December 2000) (arrows in Fig. 5c) in the gulf (Box B in Fig. 1B) from monthly average SeaWiFS images obtained during January 1999 to December 2000. Another small peak occurred in spring following the winter peak in 2000. The lowest Chl-*a* was in summer months. The annual average Chl-*a* is 0.51 mg m^{-3} in this region during these 2 years.

3.3. Water condition, winds and water temperature

The data show differences in water conditions between coastal waters (station D) and the center of the gulf

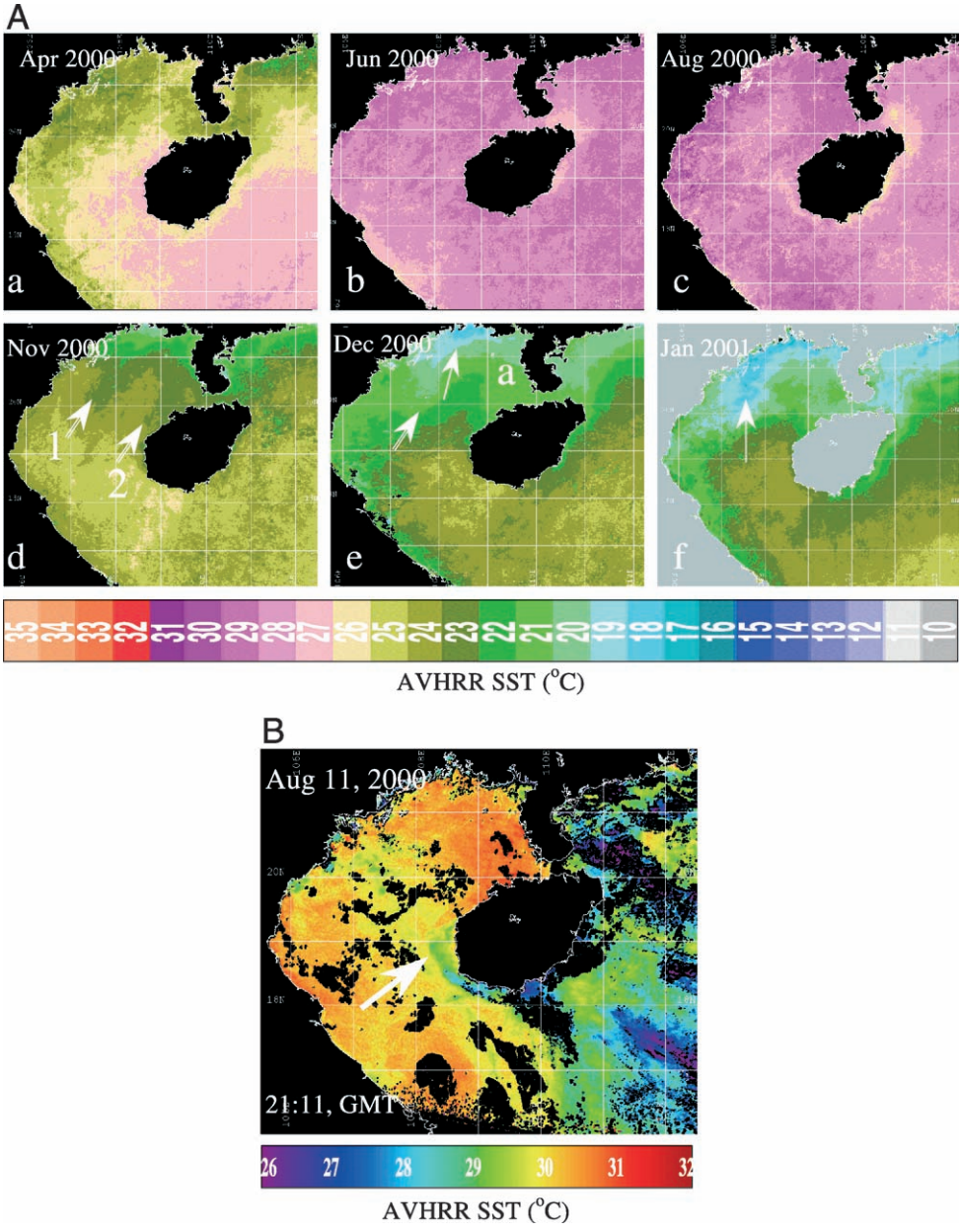

Fig. 6. (A) Monthly average AVHRR SST images in 2000. Spatial resolution is 1.1 km. Color bar indicates water temperature (°C), coastlines are shown in white color. (B) Nighttime AVHRR SST image obtained on August 11, 2000. Spatial resolution is 1.1 km. Color bar indicates water temperature (°C).

(station B) (Table 1) in summer 2000. At station D, we recorded lower salinity (13.5 ‰), and higher turbidity (5.5 FTU) than at station B. It indicates river discharge from the Red River and saltier water in the center of the Gulf. Water temperatures are similar between the two stations.

Monthly average of SST shows a seasonality of water temperature in the study area (Fig. 6A). In the summer–autumn season (June–October), SST is high (27–30 °C) and distributed evenly in the whole gulf (Fig. 6Ab,c). During the winter monsoon (November–February), spatial variation of SST appears in the gulf: SSTs are lower on the northwest part than in the southeast part with a distinct area of low SST (17–20 °C) in a tongue shape southwestward from the northeast to the center beginning in November (arrows in Fig. 6Ad–f). This SST spatial variation coincided with the Chl-*a* distribution in the north part of the gulf (Fig. 3B). April (Fig. 6Aa) is a transition month.

SST may be influenced by sea surface heating in summer therefore we analyzed nighttime SST images (August 11, 2000) and used a different color bar to display detail spatial variation of temperature. Fig. 6B shows relatively uniform temperature in the entire gulf. Low SSTs (arrow in Fig. 6B) have been observed along the Hainan Island, the same location of high Chl-*a* concentration in SeaWiFS image (arrow 2 in Fig. 5Ad) in the same month. This may indicate a regional upwelling or tidal mixing.

Monthly average wind speed and directions show a seasonal reversal monsoon in the study area in 2000 (Fig. 7). There are southwesterly winds in summer and northeasterly winds in winter. In November and December, the strong northeast winds (about 10 m/s) appear in the east part of the gulf (white circle in Fig. 7f,g), where is the location of phytoplankton blooms (Fig. 3Ad); the winds are parallel to the west coast of the Hainan Island. The winds decrease in January 2001 (Fig. 7h), and weaken from the east to the west in March (5 m/s) (Fig. 7b).

4. Discussion

4.1. Comparison Chl-a obtained from SeaWiFS and in situ measurements

Validation of satellite data is important for interpreting satellite measurements. Availability of satellite ocean color data may vary from area to area, such as from open ocean to coastal waters (Hooker & McClain, 2000; Tang et al., 1998). In Case I waters, specifications called for uncertainties less than ±5% in retrieved water-leaving radiance and less than ±35% in Chl-*a* concentration over the range of 0.05–50 mg m^{-3} (Hooker, Esaias, Feldman, Gregg, & McClain, 1992). Ocean color data may have some biases, particularly near river mouths and in shallow waters. The present study is the first analysis of SeaWiFS data with in situ measurements in the Gulf of Tonkin, which shows that SeaWiFS derived Chl-*a* values fit well with the in situ measurements in most of the gulf, including shallow water (Fig. 3C). Among these stations, station 4 is the shallowest station, where SeaWiFS data shows good comparison with in situ measurement (Fig. 4A,B). However, SeaWiFS derived Chl-*a* values are higher than in situ measurements near river mouths, such as stations 3 and 7 (Fig. 4A). Higher Chl-*a* values derived from SeaWiFS data may be caused by suspended sediment from river discharges.

In this study, although the in situ measurements are not at the same time as the satellite measurements, the comparison shows general consistency between the two data sets. SeaWiFS-derived Chl-*a* concentrations in this

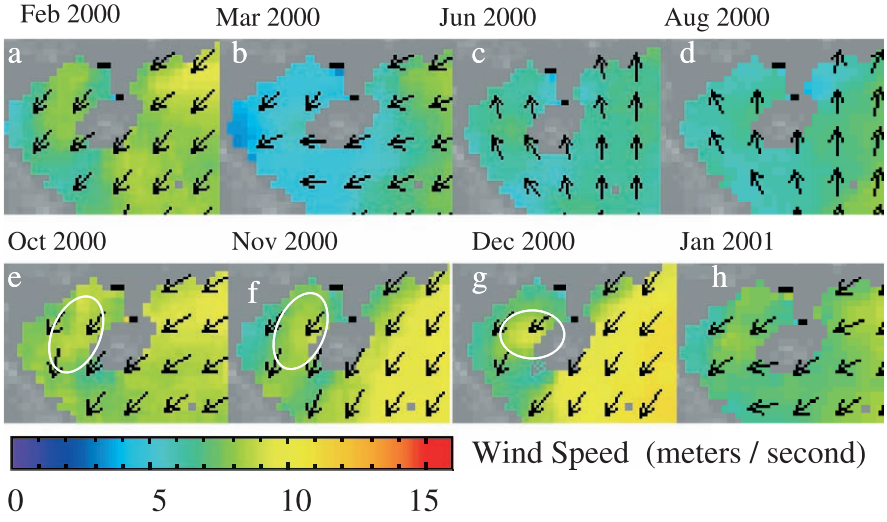

Fig. 7. Monthly averaged wind images in 2000 derived from QuikScat. Color bar indicates wind speed, and arrows show wind directions. Land regions are colored gray. Areas where QuikScat data are not available are black.

study agree with field measurements by An and Du (2000), and Suchint & Puntip (2000), and is also consistent with CZCS image obtained in 1997 (Fig. 2). SeaWiFS data help identify the spatial and monthly variation of Chl-*a* in the Gulf of Tonkin.

4.2. Seasonal and spatial distribution of Chl-a in the Gulf

The Gulf of Tonkin has characteristics of tropical mesotrophic waters, receiving relatively high energy of solar radiation that creates favorable conditions for the photosynthesis of phytoplankton (An & Du, 2000), and experiences a seasonal reversal monsoon (Shaw & Chao, 1994). The present study reveals an obvious seasonality of Chl-*a* distributions in this region.

In summer, Chl-*a* content is relative low and uniform in the whole gulf; high Chl-*a* concentrations are limited only to a narrow band along the coast (Figs. 3A and 5Ac, d). Because of weak winds and large sea surface heating, water stratification is well developed in this season, which results in relative uniform SSTs in the entire gulf for this season (Fig. 6Ab,c). This water stratification limits upwelling of nutrients and phytoplankton growth (Fig. 3A). Many regions of the world's ocean show oligotrophic conditions during the period of vertical stratification (Varela, Cruzado, Tintore, & Garcia-Ladona, 1992). High Chl-*a* content along the Vietnam coastal waters (Fig. 3A) may be due to nutrients from runoff from the coastal cities and some small rivers that discharge into the gulf (Suchint & Puntip, 2000). This agrees with our monitoring data (Table 1) that shows higher TSS and turbidity in the west coastal waters than in the center of the gulf in summer. High Chl-*a* along the western coast of Hainan Island (arrow 2 in Fig. 5Ad) may be due to regional upwelling and tidal mixing (arrow in Fig. 6B). In the Qiongzhou Strait and west coast of the Qiongzhou Peninsulas, because of strong tidal mixing with strong currents (>40 cm/s in velocity) (Huang et al., 1994), nutrients were upwelled to the surface and enhanced phytoplankton growth (Fig. 3A,B).

4.3. Phytoplankton blooms during the northeast monsoon

In winter, the Chl-*a* concentrations increase in the whole gulf, particularly in the northeast of the gulf (Figs. 2, 3B and 5Aa). This spatial variation of Chl-*a* coincides with lower SST in the northeast gulf. The most prominent feature observed in this study is the high Chl-*a* offshore from the northeast coast to the center of the gulf, not limited to the coastal waters. Water temperature and nutrients are two important factors affecting phytoplankton growth. In the gulf, solar radiation creates favorable water temperatures for phytoplankton (An & Du, 2000), and nutrients along the west coastal water were discharged from rivers (Suchint & Puntip, 2000). Therefore, the major question concerning these winter phytoplankton blooms in the center is what are the nutrient sources in the center of the gulf?

Because of the strong northeast monsoon (Fig. 7h,g) and sea surface cooling (Fig. 6d–f), stratification vanishes and vertical mixing develops in November–January. The winds parallel to the west edge of the Hainan Island (Fig. 7h,g) may cause water advection offshore-ward. The Ekman drift pushes the water offshore-ward from the east side to the center of the gulf, inducing water upward in the coastal water of the Hainan. Previous surveys show that the nutrients were higher in deep water than in the surface water in the Gulf of the Tonkin and contents of Chl-*a* have a tendency to increase with depth in the west part of the gulf (An & Du, 2000), with the Chl-*a* maximum depth range between 7 and 90 m (Suchint & Puntip, 2000). These vertically mixed and upwelled waters bring up nutrients to the surface, as well as phytoplankton from the sub-thermocline to the surface in the east part of the gulf. These nutrients can support phytoplankton blooms. When the northeast monsoon vanishes at the end of winter (Fig. 7h), this phenomenon disappears and phytoplankton blooms decrease. The distinct water mass of low temperature in the north tip of the gulf toward the center of the gulf in winter (Fig. 6Ae) matches the high content of phytoplankton in terms of location and time (Fig. 3Ae). It may indicate cold upwelled water in that region enhancing the southwestward phytoplankton blooms. The front of water in the center of the gulf may also enhance the phytoplankton bloom.

This is the first study of seasonal variation of Chl-*a* concentration in this region. Similar situation has been reported in the Arabian Sea, which also experiences reversal monsoon (Gradner, Gundersen, Richardson, & Walsh, 1999). The deepest seasonal mixing layer occurred during the northeast monsoon, which influences the distribution of Chl-*a*. Winter phytoplankton blooms were observed in the northwestern Arabian Sea (Tang, Kawamura, & Luis, 2002), which was associated with a cold eddy influenced by wind stress during winter monsoon. The northeast monsoon sets up winter bloom conditions in the Gulf of Tonkin with about the same seasonal timing as phytoplankton blooms conditions southwest off the Luzon Strait in the South China Sea (Tang, Ni, Kester, & Müller-Karger, 1999).

This winter phytoplankton bloom in the central portion of the gulf has not been noticed before, probably because previous surveys, such as SEAFDEC in May were limited to the west part of the gulf, and there is no study using satellite images covering the entire Gulf. More investigations on the water column are needed in future studies for understanding this observation.

5. Conclusion

This study illustrates seasonal and spatial variations of Chl-*a* concentration and the other water parameters in the Gulf of Tonkin. The seasonality of Chl-*a* is related to reversal seasonal monsoon via the changes of water conditions. There is one peak of Chl-*a* concentration per year,

which occurs during northeast monsoon. In summer, Chl-*a* concentrations are low and relatively uniform; this is related to water stratification caused by sea surface heating. In winter, Chl-*a* concentration increase in the entire gulf, and phytoplankton blooms southwestward to the center of the gulf; this is associated with water advection westward toward the center of the gulf from the coastal area drawn by Ekman drift during strong northeast monsoon; it may also be related to water vertical mixing and tidal mixing. The results indicate that nutrient supply from the river discharges is important for phytoplankton growth in the coastal water, but the nutrient up-take from the bottom layer contributes to phytoplankton growth in the center area.

This study also compares Chl-*a* values between SeaWiFS-derived and in situ measurements in the Gulf of Tonkin. These two data sets fit well and show the same tendency of Chl-*a* changes in this study region including shallow waters except near river mouths.

Acknowledgements

This study is supported by "Special Coordination Funds for Promoting Science and Technology" of MEXT Japan, and a fund from the National Space Development Agency of Japan (NASDA) through a grant to the Asian I-Lac Project at Tohoku University in 2000. Dr. M-A. Lee's work was supported by the National Science Council through Keelung Station of National Center of Ocean Research in National Taiwan Ocean University. In situ Chl-*a* were measured by Department of Marine Science, Kasetsart University, Thailand; water monitoring data were provided by Haiphong Institute of Oceanography and Interdepartmental Collaborative Research Program SEAFDEC. QuikScat data are produced by Remote Sensing Systems and sponsored by the NASA Ocean Vector Winds Science Team. We extend great appreciation to Professor Dana R. Kester of the University of Rhode Island, for his valuable comments and suggestions. We thank Mr. Wataru Takahashi and Mr. Takuya Ohnishi of Tohoku University, and Miss Jui-Wen Chan of National Taiwan Ocean University for their assistance in computer programming.

References

An, N. T., & Du, H. T. (2000). Studies on phytoplankton pigments: chlorophyll, total carotenoids and degradation products in Vietnamese waters. *Proceeding of the SEAFDEC seminar on fishery resources in the South China Sea area IV: Vietnamese water* (pp. 1–18). Thailand: Southeast Asian Fisheries Development Center.

Emery, W. J., Thomas, A. C., Collins, M. J., Crawford, W. R., & Mackas, D. L. (1986). An objective method for computing advective surface velocities from sequential infrared satellite images. *Journal of Geophysical Research*, *91*(C11), 12865–12878.

Gradner, W. D., Gundersen, J. S., Richardson, M. J., & Walsh, I. D. (1999). The role of seasonal and diel changes in mixed-layer depth on carbon and chlorophyll distributions in the Arabian Sea. *Deep-Sea Research, II*, *46*, 1833–1858.

Hooker, S. B., & McClain, C. R. (2000). The calibration and validation of SeaWiFS data. *Progress in Oceanography*, *45*(3–4), 427–465.

Hooker, S. B., Esaias, W. E., Feldman, G. C., Gregg, W. W., & McClain, C. R. (1992). An overview of SeaWiFS and ocean color. In S. B. Hooker, & E. R. Firestone (Eds.), *NASA Tech. Memo., vol. 1* (p. 104566). Greenbelt, MD, USA: NASA Goddard Space Flight Center.

Huang, Q. Z., Wang, W. Z., & Chen, J. C. (1994). Tides tidal currents and storm surge set-up of South China Sea. In D. Zhou, Y. B. Liang, & C. K. Zeng (Eds.), *Oceanology of China seas* (pp. 113–122). AH Dordrecht, The Netherlands: Kluwer Academic Publishing.

Hsu, C. -H., Lee, K. -T., Lee, M. -A., Liao, C. -H., & Lu, H. -J. (2000). Effects of seasonal environment changes on the mackerel purse seine fishery in the waters off northeast Taiwan monitored by satellite remote sensing. *Proceedings of the joint Taiwan–Australia aquaculture and fisheries resource and management forum* (pp. 257–261). Keelung, Taiwan: Taiwan Fish. Res. Inst.

Kubota, M. (1994). A new cloud detection algorithm for nighttime AVHRR/HRPT data. *Journal of Oceanography*, *50*, 31–41.

NASA (2001). Available at: http://www.ssmi.com/qscat/qscat_description.html.

O'Reilly, J. E., Maritorena, S., Mitchell, B. G., Siegel, D. A., Carder, K. L., Garver, S. A., Kahru, M., & McClain, C. (1998). Ocean color chlorophyll algorithms for SeaWiFS. *Journal of Geophysical Research*, *103*, 24937–24953.

Penjan, R., Siriporn, P., Natinee, S., & Somboon, S. (2000). Temperature, salinity, dissolved oxygen and water masses of Vietnam waters. *Proceeding of the SEAFDEC seminar on fishery resources in the South China Sea area IV: Vietnamese water* (pp. 346–355). Thailand: Southeast Asian Fisheries Development Center.

Shaw, P. T., & Chao, S. Y. (1994). Surface circulation in the South China Sea. *Deep Sea Research*, *41*(11/12), 1663–1683.

Simpson, J. J., & Humphrey, C. (1990). An automated cloud screening algorithm for daytime Advanced Very High Resolution Radiometer imagery. *Journal of Geophysical Research*, *95*(C8), 13459–13481.

Suchint, D., & Puntip, W. (2000). Sub-thermoline chlorophyll maximum in the South China Sea. *Proceeding of the SEAFDEC seminar on fishery resources in the South China Sea Area IV: Vietnamese water* (pp. 1–17). Thailand: Southeast Asian Fisheries Development Center.

Tang, D. L., & Kawamura, H. (2002). Ocean color monitoring of coastal environments in the Asian waters. *Journal of the Korean Society of Oceanography*, *37*(3), 154–159.

Tang, D. L., Kawamura, H., & Luis, A. J. (2002). Short-term variability of phytoplankton blooms associated with a cold eddy on the North-western Arabian Sea. *Remote Sensing of Environment*, *81*(1), 82–89.

Tang, D. L., Kester, D. R., Ni, I. -H., Kawamura, H., & Hong, H. S. (2002). Upwelling in the Taiwan Strait during the summer monsoon detected by satellite and shipboard measurements. *Remote Sensing of Environment*, *83*, 457–471.

Tang, D. L., Ni, I. -H., Kester, D. R., & Müller-Karger, F. E. (1999). Remote sensing observation of winter phytoplankton blooms southwest of the Luzon Strait in the South China Sea. *Marine Ecology. Progress Series*, *191*, 43–51.

Tang, D. L., Ni, I. -H., Müller-Karger, F. E., & Liu, Z. J. (1998). Analysis of annual and spatial patterns of CZCS-derived pigment concentrations on the continental shelf of China. *Continental Shelf Research*, *18*, 1493–1515.

Varela, R. A., Cruzado, A., Tintore, J., & Garcia-Ladona, E. (1992). Modelling the deep-chlorophyll maximum. A coupled physical-biological approach. *Journal of Marine Research*, *50*, 441–463.

Wentz, F. J., Smith, D. K., Mears, C. A., & Gentemann, C. L. (2001). Advanced Algorithms for QuikScat and SeaWinds/AMSR. *IGARSS'01 proceedings 2001* (pp. 1–3). USA: NASA.